

# National-wide deep-seated landslide mapping and susceptibility update via airborne laser scanning raster data and InSAR analysis in Taiwan

Cartographie nationale de glissement de terrain de type profond et mise à jour de susceptibilité via des données raster de balayage laser aéroportées et des analyse InSAR à Taiwan

Titre du document en Français

Ching-Fang Lee , Wei-Kai Huang

*Disaster Prevention Technology Research Center, Sinotech Engineering Consultants, INC., Taipei, Taiwan, R.O.C.*

Shih-Yuan Lin

*Department of Land Economics, National Chengchi University, Taipei, Taiwan, R.O.C.*

Cheng-Lung Chiu, Chung-Chi Chi

*Environmental & Engineering Geology Division, Central Geological Survey, MOEA., New Taipei City, Taiwan, R.O.C.*

**ABSTRACT:** Extreme rainfall with long-term period plays a principal role in triggering deep-seated landslide around the mountainous area. A well-known typhoon Morakot, the most destructive event occurred in August 2009, battered southern Taiwan and caused severe casualties in Siaolin Village. To reduce the damage and to prevent loss of life resulting from the catastrophic landslide, this study adopted high-resolution topographic data which extracted from airborne LiDAR scanning to interpret both recent and ancient deep-seated landslides in northern, central, southern, and eastern Taiwan (2015-2018). Firstly, a relief visualization technique called sky-view factor was utilized to generate the quasi-3D map by overlapping slope gradient, and multiple direction hillshading maps, allowing one to interpret manually detailed landslide topography and assess the hazard potential. The study area of the on-going project covers an area of 17,000 km<sup>2</sup>. This study recognized main scarp and landslide body in polygon pattern by landslide micro-topography interpretation; it showed more than 700 deep-seated landslides were mapped and located on Central Range and Western foothills in Taiwan. This work also uses the recent surface deformation of multi-stage InSAR analysis to update landslide susceptibility. Furthermore, the result of the study will contribute to upgrading the national-wide environmental geologic map and provide competent authority to make decisions reducing the geohazard risk.

**RÉSUMÉ:** Les précipitations extrêmes à longue terme jouent un rôle essentiel dans le déclenchement de glissement de terrain de type profond près des régions montagneuses. Le typhon Morakot, l'évènement le plus dévastateurs survenu en Août 2009, a frappé le Sud de Taiwan, causant de nombreuses victimes dans le village de Siaolin. Pour réduire les dégâts et prévenir les pertes en vie humaines résultant des glissements

catastrophique de terrain, cette étude a adoptée des données topographiques à haute résolution extraites des balayages LiDAR aéroportés afin d'interpréter les récents et anciens glissements de terrain de type profond dans le Nord, le Centre, le Sud et l'Est de Taiwan (2015-2018). Premièrement, une technique de visualisation en relief appelée 'Sky-view factor' a été utilisée pour générer une carte quasi-3D en superposant le gradient de la pente, ainsi que des cartes d'ombrage dans plusieurs directions, permettant d'interpréter manuellement la topographie détaillée de glissement de terrain et d'évaluer les dangers potentiels. L'étude du projet en cours couvre une superficie de 17000km<sup>2</sup>. Cette étude a permis de reconnaître l'escarpement principal et les formes associées à ces glissements de terrain grâce à l'interprétation de la microtopographie de glissements de terrain; elle a aussi montré que plus de 700 glissements de terrain de type profond ont été cartographiés et situés sur les contreforts de la chaîne centrale et occidentale de Taiwan. Ce travail utilise également l'analyse échelonnée de déformation de surface récente InSAR pour la mise à jour de susceptible glissements de terrain. En outre, les résultats de l'étude contribueront à actualiser la carte géologique de surveillance environnementale à l'échelle nationale et permettront à l'autorité compétente de prendre des décisions pour réduire les risques des aléas géologiques.

**Keywords:** deep-seated landslide; LiDAR; sky-view factor; landslide micro-topography interpretation; PS-InSAR.

## 1 INTRODUCTION

In a subtropical and tropical area of western Pacific, the rainfall of typhoon is much higher, resulting in many sediment-related disasters. Deep-seated landslide, which characterized by large-range deposition area and sediment volume, can be considered as a critical natural disaster in the remote area around the world. To identify the landslide-prone regions, several landslide mapping approaches by semi-automatic and manually identifications were developed in the decades (Van Den Eeckhaut, 2013; Nonomura, 2013; Petschko, 2016). Several remote sensing techniques such as LiDAR (Light Detection and Ranging), InSAR, and UAV survey are also applied to detect and interpreting regional landslide in advanced. Concerning deep-seated landslide, the location is usually covered with dense forest in subtropical zone and difficult to map the exact terrain boundary of the landslide on aerial or satellite image. Identification of deep-seated landslide pattern suggests that high-resolution digital terrain model (after removing the vegetation on the ground) is one of the best

topographical data. Several studies have shown that landform enhancement on the shading relief map is a practical approach for micro-relief structures of mapping slope-land related natural hazards (Yokoyama, 2002; Zakšek, 2011). For enhancing surface features in the landslide-prone area, the landslide micro-topography interpretation is performed by using the combination of analytical hill-shading in multiple directions, slope gradient, color cast, and openness (positive and negative) visualizations. The application of three-dimensional visualization facilitates manual interpretation and digitalizing precision in comparison with using a single relief map.

This project supported by Central Geological Survey (CGS), MOEA divides Taiwan into four main regions covering the northern (2015), southern (2016), central (2017), and eastern (2018) Taiwan. This paper focuses on the whole of Taiwan, which contains 137 map sheets with 1/25,000 scale generated by airborne LiDAR scanning during 2010 and 2015. The primary purpose of this project includes two aspects: establishing national-wide deep-stead landslide inventory and assess the reactivation of old

landslides. Both expert-based interpretation and on-site survey are the main analytical process for landslide mapping and susceptibility classification. A generation procedure of sky-view factor relief map will be first applied to replace the traditional 8-directions hill-shading on high-resolution DTMs.

Moreover, the feature of the deep-seated landslide is extracted to identify its pattern and boundary. Surface deformation derived from PS-InSAR (Persistent Scatterer Interferometric Synthetic Aperture Radar) is also produced to assess the recent reactivation of the old landslides. This visualization result can provide the fundamental data for updating the environmental geological map and assist in deciding the proper site with high priority for establishing a long-term monitoring system.

## 2 STUDY AREA

Taiwan is located in the western Pacific Ocean, at the convergent plate boundary zone of Philippine Sea plate and Eurasian plate, causing hundreds of faults and folds due to tectonic activity (Fig. 1(a)). The topography in the study area consisted mostly of the basin, plain, volcano, plateau, and mountain region (Fig. 1(b)). The coastal plain gains the height of Central Range at an elevation between 10 m (western plain) to 3,952 m (Central Range).

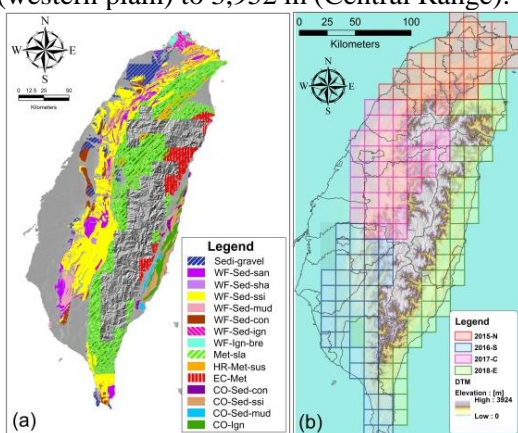


Figure 1. (a) Geological settings in Taiwan and (b) study area in northern (2015), southern (2016), central (2017), and eastern (2018) Taiwan

According to the official geological map, the geological setting of the study area contains sedimentary rock, pyrogenetic rock, metamorphic rock, slate, volcanic breccia, and conglomerate. Rainfall statistics analysis of Taiwan shows the annual averaged rainfall and rainfall day are 2,500 mm and 120 days, respectively. Due to the high population density (647 population/km<sup>2</sup>) and the frequent occurrence of natural disasters, the World Bank reported that Taiwan is one of the most high-risk countries around the world.

## 3 MATERIAL AND METHODOLOGY

### 3.1 High-resolution DEMs

After the sediment-related disaster of Typhoon Morakot, Central Geological Survey launched the project, which was entitled: “Investigation and analysis for the geologically sensitive area in the national preservation domain program” from 2009 to 2015. This national program adopted the wide-range airborne LiDAR technique to generate DEMs of 1 m spatial resolution in a metropolitan and mountainous area covering the whole of Taiwan. For the demand of the application, the corresponding mean cloud density in the alpine zone is at least 2 points/m<sup>2</sup>.

All the produced LiDAR derivatives such as DSM and DEM are separated into individual map sheets with 1:5000 scales for regional geohazard assessment. Fig. 2 shows the workflow of this study; it includes three parts: data acquisition, data production, and the referenced map overlay. Beyond the dataset of DEMs mentioned above, environmental geological map, disaster potential map, orthophoto image (e.g., Google Earth and aerial image available), and landslide inventory are also included. Finally, the result of work will be

involved to update the inventory and landslide susceptibility with combining surface displacement (LoS) of the PS-InSAR.

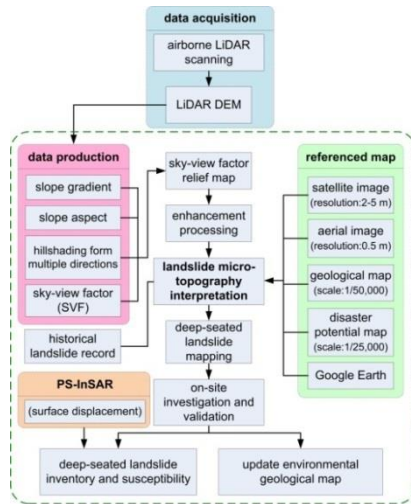


Figure 2. workflow of the study

### 3.2 SVF relief map

Conceptually similar to topographic openness, diffuse illumination can be adopted in relief maps to address the shadowing effect caused by a light source from a single direction (Zakšek, 2011). The SVF (sky view factor) can be regarded as a virtual light source within a hemisphere situated at the center of the point of illumination. The definition of SVF follows the assumptions: (1) uniform light throughout the hemisphere, (2) no other sources of light, and (3) disregard of any changes in the curvature of the Earth within a 10 km radius. Fig. 3 illustrates the procedure used in the compilation of the SVF relief map, which first involved compiling a slope map and then an SVF map by using the LiDAR DEMs. In layering the maps together, changes in elevation are enhanced, and noise is removed as needed. The result is a monochrome SVF relief map, which is then combined with a color elevation map to produce a colored SVF relief map. Fig. 3 demonstrates relief maps of the landslide area before the disaster, which was compiled using the proposed approach. The

steeper terrain on SVF relief map is displayed in darker tones, whereas gentler slopes are presented in lighter tones. The flat river terrace or alluvial fan even shows a micro-drainage system, and the bulging mountain ridgelines (lighter tones) and recessed ravines (darker tones) are also more clearly discernible. The using of SVF relief map instead of hill-shading in 8 directions will advantage geologic experts to interpret fundamental characteristic of the landslide (scarp, ridge, and streamline), and reduce the analysis time of mapping by utilizing an only single relief map.



Figure 3. SVF relief map compilation procedure

### 3.3 Mapping criteria for deep-seated landslide

Central Geological Survey in Taiwan categorizes landslide behavior into three main types based on slope movement classification: (1). debris slide (shallow landslide), (2). rockfall, and (3). rock slide (deep-seated landslide). Generally speaking, deep-seated landslide means a landslide process characterized by large-scale slope movement and deep-seated sliding plane. The surface of rupture for this slope movement usually appears beneath the bedrock, so that one can observe specific terrain features at different parts of landslide zonation (Fig. 4; Central Geological Survey, 2010). The mapping principle in the study follows the definition of rock slide which was announced by CGS. For typical deep-seated landslide in the field, a deep sliding plane, thick slope movement, and large-scale sediment volume often coexist and can be interpreted on the

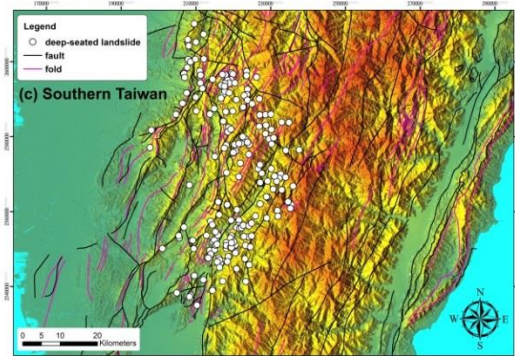
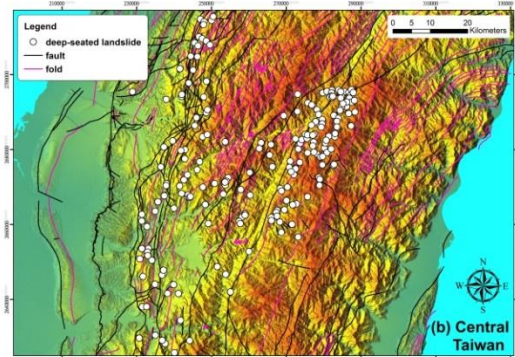
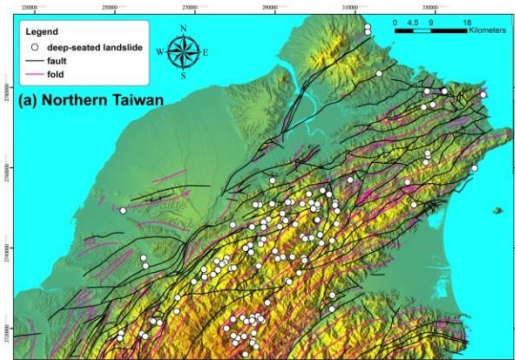
visualization map. The scale of the landslide area even reaches more than 10 hectares, but the main body still preserves its integrity during the sliding process. Regarding the type of movement, deep-seated landslide comprises translational, rotational, and complex slides. Large-scale deep-seated landslide is usually triggered by translational slide located on the dip slope in Taiwan - Tsaoling, and Chiufengershan for example. All the characterization and the types which for extracting landslide feature from LiDAR derivatives are adopted into expert-based interpretation approach. Moreover, the corresponding criterion such as discordant vegetation for remote sensing on landslide feature is also taken into consideration. Eventually, the interpretation results obtained with this process will be validated by three experts to reduce the misinterpretation.

bedrock landslides are distributed along the strike of the bedrock in west Taiwan, and most landslides are within the Central Range; a high elevation northeast-southwest oriented range of mountains. Moreover, a few landslides are also clustered along the edge of the Datun volcano group and near the western foothills. The mapping results indicate that location of deep-seated landslide and geological structure (fault and fold) are highly relevant.

## 4 RESULTS AND DISCUSSIONS

### 4.1 Deep-seated landslide mapping

Based on the visualization SVF relief map, deep-seated landslides mapped using micro-topographic interpretation by experts in 2,764 map sheets (with 1:5000 scale) are completed. In the preliminary statistics, 740 landslide areas are mapped and are shown in Fig. 4(a)-(d) within the study area. An example of detailed deep-seated landslide feature is shown in Fig. 5. The mapped areas include the main scarp and landslide body primarily. Fig. 6 indicates the statistical analysis of mapped landslide area for northern, central, and southern Taiwan. The mean area of each mapped target is approximately 10.8 ha, which satisfies with the “greater than 10 ha” criteria of classic deep-seated landslides by National Science and Technology Center for Disaster Reduction (NCDR). The mapping result shows most landslides are located around Hsuehshan Range, Central Range, and western foothills. Based on results of bedrock landslide mapping, most



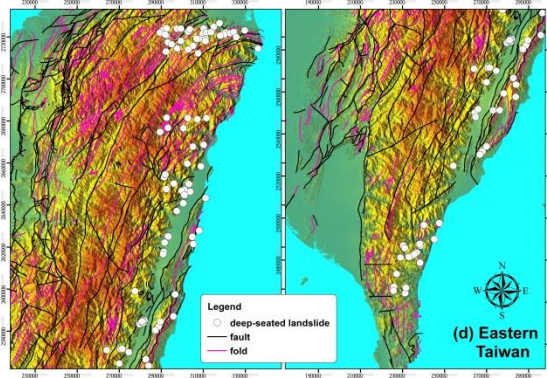


Figure 4. Deep-seated landslide mapping in the study area: (a) northern (122 landslides; 800 sheets), (b) central (235 landslides; 1010 sheets), (c) southern (262 landslides; 954 sheets), and (d) eastern (121 landslides; 813 sheets) Taiwan

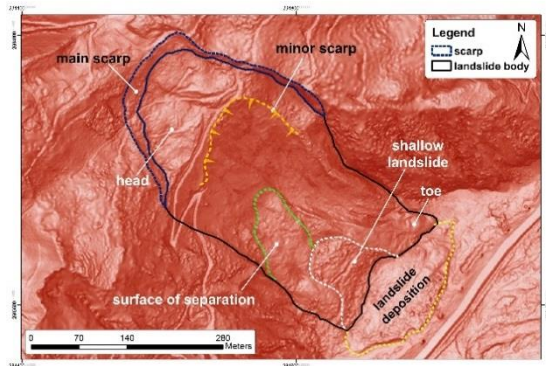


Figure 5. Illustration of main scarp and landslide body of the deep-seated landslide in central Taiwan

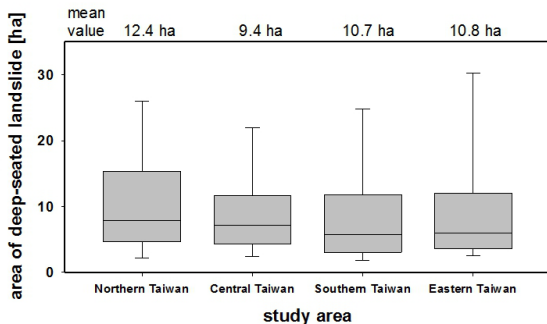


Figure 6. The box plot of deep-seated landslide area in different regions of Taiwan

## 4.2 Landslide activity assessment

The failure mechanism of deep-seated landslide is affected by geologic setting, topography and hydrologic conditions. In term of failure process and displacement, typical failure patterns include (1) regressive failure; (2) progressive failure; (3) translational failure. Regarding deep-seated landslides, unless the failure behavior begins once as a single, catastrophic landslide, initial failure occurs near the crown or head of the landslide, and the unstable landslide mass remains parked on the failure plane. It is likely if topography below the slide is constrictive or the slope on which the mass movement is occurring is low. If no other triggering factors exist, the landslide can transition from an active to suspended or dormant state for a long time. Provided that the dormant landslide is affected by some other outside triggering factors such as rainfall or earthquakes, the landslide may become active again. Once it activates, the sliding mass can remobilize, stop and separate into a debris deposition.

To further understand the mapped deep-seated landslides in Taiwan, the possible active landslides and the reactivation potential of landslides is assessed by considering remote sensing imagery analysis, topographic characteristics, and on-site monitoring records.

To further understand the mapped deep-seated landslides in Taiwan, the possible active landslides and the reactivation potential of landslides is assessed by considering remote sensing imagery analysis, topographic characteristics, and on-site monitoring records. In this project, we established a reactivation rating approach for deep-seated landslides using two-dimension metrics which called risk matrix: topographic features and recent landslide activities (Fig.7). Topographic characteristics include the micro-topographic characteristics of the landslide head, body, and toe (Tab.2). Besides, the current landslide activities will be

evaluated by multiple-stage PSI acquired from satellite-based radar image.

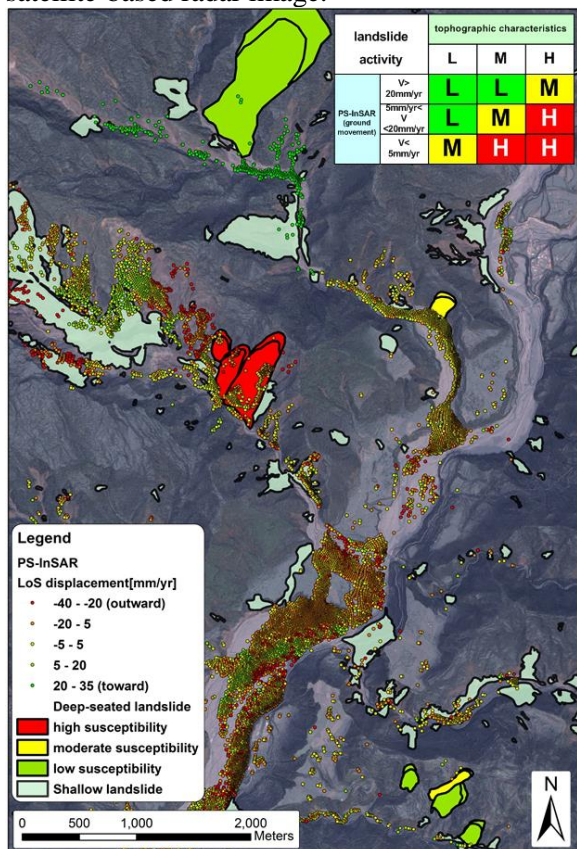


Figure 7. The results of deep-seated landslide activity assessment which combines topographic characteristics and recent ground movement.

Table 2 Hillslope topographic characteristics used for remote-sensing interpretation of deep-seated landslides

Susceptibility	Terrain features
Low	<b>Scarp</b> and <b>main body</b> of landslide can be identified and mapped. Deep-seated gravitational slope deformation is limited to the peak or ridgeline of the slope.
Moderate	<b>crown and head:</b> The scarp is rounded or muted, suggesting the scarp is not fresh. Additionally, the landslide body contains two stream channels which originate from a single location. Also, abnormal openings in the forest canopy are discernible in images of the landslide.
	<b>main body:</b> located on a dip slope, gullies are well defined and dense, multiple areas of debris, secondary scarps or reverse scarplets.

	<b>foot and toe:</b> A stream or road cuts across the foot of a dip slope; the toe of the landslide is less constricted than the head; evidence of debris slides.
	<b>recent observation:</b> Observation of movement has been recorded in the landslide inventory within the last 20 years.
High	<b>crown and head:</b> Tension cracks are located upslope of the scarp and the scarp is fresh and shows signs of recent formation.
	<b>main body:</b> The head is step-like, hummock and the landslide mass is cracked and fissured. The vegetative cover is disturbed.
	<b>foot and toe:</b> The foot and toe are adjacent to high-energy, rapidly scouring reach of the stream; the edge adjacent to the stream shows signs of instability.
	<b>recent observation:</b> If a monitoring system is installed, recent movement has been recorded.

For the first part, each deep-seated landslide is evaluated using topographic conditions as well as several other indicators of potential instability (Table 2). Additionally, multi-temporal imagery available on Google-Earth is used to verify interpreted irregularities in the vegetation on the landslide zonation. Recent landslide signs of activity are also checked from PS-InSAR analysis during the 2015/06-2017/02. For landslides that already installed landslide monitoring systems, the mobilization of the landslide history is directly validated from the monitoring record.

Secondly, PS Interferometry (PSI) is the multi-interferometric SAR technique often adopted in ground deformation with millimeter accuracy. We defined three class for assessing landslide activity according to the mean annual surface deformation on the hillslope as high ( $V > 20$  mm/yr), moderate ( $5 \text{ mm/yr} < V < 20 \text{ mm/yr}$ ), and low levels ( $V < 5 \text{ mm/yr}$ ). To determine how may PSI and terrain features can be used to evaluate landslide susceptibility, risk matrix by two-dimension indices is considered. An example of the landslide activity result is shown in Fig. 7. The Results reveal that most landslides are located in a complicated geologic setting, such as fault and fold zones or areas of bedding contacts and regions of highly weathered rock. The landslide areas characterized by high activity show signs of landslide topography like

as perched areas of loose debris and steep scarps that have a higher potential to fail. Under intense rains, these would usually re-activate rapidly. If infrastructure or residential houses are located at the foot of these areas, they would require particular attention and prioritization for evacuation planning.

## 5 CONCLUSIONS

This study attempt using high-resolution LiDAR data and mapping deep-seated landslide-prone area on the national-wide scale. SVF relief maps are verified well to extract the landslide micro-topography and drainage characteristics instead of 8-direction hillshading relief for the mountainous region. The main scarp and landslide body were interpreted manually, and in total, 740 landslides were identified. The average area of the deep-seated landslide in different geological zonation is 10.8 ha in Taiwan. The result of this study pointed out the exact hotspot of possible geo-hazard on the hillslope; it may help to make a proper decision to set monitoring system and disaster prevention before the occurrence of the landslide. Furthermore, a long-term slowly deformation of deep-seated landslide could be acquired by InSAR techniques. With that dataset and the flowchart we proposed, the destructive consequence of catastrophic landslides around remote villages could be highly prevented and reduced in advance.

## 6 ACKNOWLEDGEMENTS

The authors would like to thank the Central Geological Survey, MOEA, Taiwan, for supporting this research financially and providing insightful comments on the project.

## 7 REFERENCES

Central geological survey, 2010. Geological hazard assessment and monitoring in

mountain area. Central geological survey, MOEA, Taiwan (in Chinese).

Lee, C.F., Huang, W.K., Chiu, C.L., Chi, C.C. 2018. Inventory mapping, geomorphic characterization, and validation of deep-seated landslides using sky-view factor visualization: northern, central, and southern Taiwan. *Proceedings, Gi4DM conference*, (Eds: Tanzi, T), 319-325, ISPRS, *Istanbul, Turkey*.

Nonomura, A., Hasegawa, S., Dahal, R.K., Chiba, T., Tadono, T., 2013. A mapping method of deep-seated landslide susceptible slopes using digital elevation model. *International Journal of Landslide and Environment* **1**(1), 67-68.

Petschko, H., Bell, R., Glade, T., 2016. Effectiveness of visually analyzing LiDAR DTM derivatives for earth and debris slide inventory mapping for statistical susceptibility modelling. *Landslides* **13**(5), 857-872.

Van Den Eeckhaut, M., Kerle, N., Hervas, J., Supper, R., 2013. Mapping of landslides under dense vegetation cover using object-oriented analysis and LiDAR derivatives. *Landslide Science and Practice*, (Eds: Margottini, C.) 1,103-109.

Yokoyama, R., Shirasawa, M., Pike, R.J., 2002. Visualizing topography by openness: A new application of image processing to digital elevation models. *Photogrammetric Engineering and Remote Sensing* **68**, 257-265.

Zakšek, K., Oštir, K., Kokalj, Ž., 2011. Sky-View factor as a relief visualization technique. *Remote Sensing* **3**, 398-415.